THE JOURNAL OF PHYSICAL CHEMISTRY C

Article

pubs.acs.org/JPCC

Quantum Dot Light-Emitting Diode Using Solution-Processable Graphene Oxide as the Anode Interfacial Layer

Di-Yan Wang,[†] I-Sheng Wang,[‡] I-Sheng Huang,[‡] Yun-Chieh Yeh,[†] Shao-Sian Li,[†] Kun-Hua Tu,[†] Chia-Chun Chen,*[,‡,§] and Chun-Wei Chen*[,†]

[†]Department of Materials Science and Engineering, National Taiwan University, Taipei 10617, Taiwan

[‡]Department of Chemistry, National Taiwan Normal University, Taipei 11677, Taiwan

[§]Institute of Atomic and Molecular Sciences, Academia Sinica, Taipei 10617, Taiwan

Supporting Information

ABSTRACT: In this article, the solution processable graphene oxide (GO) thin film was utilized as the anode interfacial layer in quantum dot light emitting diodes (QD-LEDs). The QD-LED devices (ITO/GO/QDs/TPBi/LiF/Al) were fabricated by employing a layer-by-layer assembled deposition technique with the electrostatic interaction between GO and QDs. The thicknesses of GO thin films and the layer number of CdSe/ZnS QD emissive layers were carefully controlled by spin-casting processes. The GO thin films, which act as the electron blocking and hole transporting layer in the QD-LED devices, have demonstrated the advantage of being compatible with fully solution-processed fabrications of large-area printable optoelectronic devices.

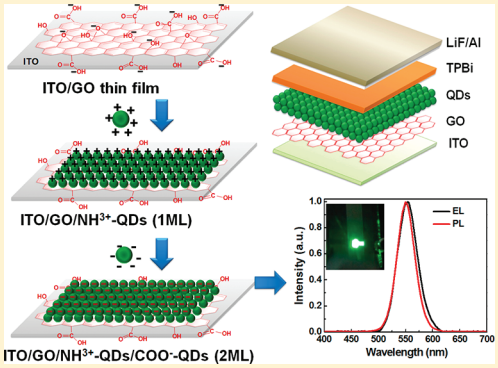

1. INTRODUCTION

Solution processable quantum dot (QD) light-emitting diodes (QD-LEDs) have demonstrated many unique advantages in optoelectronic device applications such as tunable luminescence characteristics by the quantum confinement effect and large-area low-cost fabrications.[1−6] Recently, many semiconducting QD-LEDs with promising emitting efficiencies in the visible and infrared spectral ranges have been demonstrated.[7−9] One important parameter in determining the electroluminescence (EL) efficiencies of QD-LED devices is the adequate choice of electron transporting layer (ETL) and hole transporting layer (HTL), providing balanced electron and hole injection into QD layers and stabilizing the device performance. The most popular electron transporting layers and hole transporting layers in QD-LED devices are usually based on organic molecular materials while the degradation of the organic layers largely limits the operating lifetime of QD-LED devices.[10] Recently, the replacement of charge transporting layers using more stable inorganic materials has been realized.[11,12] For example, the transparent p-type NiO_x thin films from sputtering deposition can be used as a hole transporting layer replacing the commonly used *N*,*N*-diphenyl-*N*,*N*-bis(3-methylphenyl)-1,1′-biphenyl-4,4′-diamine (TPD) organic thin film, and these devices exhibit promising electroluminescence performances.[11,12] In this work, we would like to demonstrate the incorporation of solution processable graphene oxide (GO) into QD-LEDs as the anode interfacial layer for hole transporting, which has the advantage of being fully integrated into the fabrications of printable optoelectronics over large areas.

2. EXPERIMENTS

2.1. Synthesis of Graphene Oxide. A high concentration of 67.5 mL of H_2SO_4 (purity 96%) was added into the mixture of 2.5 g of graphite powder and 1.5 g of $NaNO_3$ (purity 99%), and then the mixture was cooled to 0 °C. A 9 g portion of $KMnO_4$ (purity 99%) was gradually added within 1 h. The ice-bath cooling was kept for 2 h, and the mixture was allowed to stand for five days at approximately 20 °C with gentle stirring. In purification, to wash out the excess reactant, 1000 cm^3 of 5 wt % H_2SO_4 aqueous solution was added to the resultant mixture and stirred for 2 h. Afterward, 30 g of H_2O_2 (30 wt % aqueous solution) was added to reduce the excess $KMnO_4$. Also, manganese ions were removed by repeat washes with aqueous solution of 3 wt % H_2SO_4/0.5 wt % H_2O_2. Finally, as-prepared graphene oxide was dispersed in the DI-water for further fabrication of the hole transporting layer.

2.2. Synthesis of CdSe/ZnS QDs. A 0.2 mmol portion of CdO and 4 mmol of $Zn(acetate)_2$ were mixed with 5 mL of oleic acid (OA) in a 100 mL flask, heated to 150 °C, and kept for 30 min. Then, 15 mL of 1-octadecene (ODE) was added in the flask and heated up to 300 °C under N_2 condition to obtain a clear mixture solution of $Cd(OA)_2$ and $Zn(OA)_2$. At the

Received: October 20, 2011
Revised: April 21, 2012
Published: April 21, 2012

   dx.doi.org/10.1021/jp210062x | J. Phys. Chem. C 2012, 116, 10181−10185

temperature of 300 °C, 2 mL of TOP containing 0.1 mmol of Se and 4 mmol of S was rapidly injected into the reaction flask and reacted for 10 min. Then, the reaction was completed when reaction temperature was cooling to room temperature. The obtained QDs were purified by washing with excess amount of acetone and then dissolving in chloroform repeatedly 3 times. Finally, the QDs were dispersed in chloroform for further experiments.

2.3. Surface Modification of QDs. A 0.1 g sample of QDs dispersed in 5 mL of chloroform was transferred to water (5 mL) containing 1 g of cysteamine (NH_3^+) or mercaptopropinic acid (COO^-) by sonicating the two-phase mixture (chloroform and water) at room temperature for 1 h. Then, the QD dispersions in the water phase were purified by washing with water and adding an excess amount of acetone 5 times to remove residual surfactants. The obtained NH_3^+-QDs and COO^--QDs were finally dispersed in pH 6 and pH 8 water at different concentration, respectively.

2.4. Characterizations. High-resolution transmission electron microscopy (TEM) (HR-TEM) images were obtained using a Philips Technai G2 (FEI-TEM) microscopy operating at 200 kV. The surface roughness of the GO thin films was obtained using a AFM measurement module (Innova, Vecco Inc.). The zeta potentials of GO and QDs were measured by a Malvern Zetasizer 3000 HS. The HOMO of GO were determined by a Riken Keiki AC-2 photoelectron emission. The Current−voltage−luminescence (I−V−L) and EL spectra were measured and recorded by EL-1003 (Precise Gauge).

3. RESULTS AND DISCUSSION

Graphene oxide (GO) is a graphene sheet functionalized with oxygen functional groups in the form of epoxy and hydroxyl groups attached on the basal plane or decorated at the edges.[13−15] GO thus contains a large fraction of sp^3 hybridized carbon atoms bound to oxygen which makes it an insulator (sheet resistance ~10^9 Ω/□) with a large band gap.[16] Recently, the utilization of GO as hole transporting layer in organic photovoltaics (OPVs) was demonstrated.[17] Figure 1a shows the typical transmission electron microscopy (TEM) image of a GO sheets in the as-prepared suspension. Besides, the representative atomic force microscope (AFM) image of a GO thin film by spin-coating the GO suspensions on Si substrate was shown in Figure 1b. The lateral dimensions of GO flakes ranged from 1 to 10 μm, and the average thickness of GO film was estimated to be ~2 nm. The rms roughness of this GO film has a small value of 0.7 nm, indicating that the deposition of GO film can also assist the planarization of the ITO electrode with a rms roughness of ~3 nm.[17] In this work, the device structure of QD-LEDs consisting of ITO/GO/QDs/TPBi/LiF/Al is shown in Figure 2a, where GO and TPBi layers act as anode interfacial layer and electron transporting layer, respectively. The typical device area is about 0.05 cm^{-2}. The CdSe/ZnS QDs were prepared by wet solution chemical syntheses with some modifications.[6,18] Figure 2b shows the TEM image of the as-synthesized QDs capped with oleic acid with an average diameter of ~7 ± 1.5 nm. The high resolution TEM (HRTEM) image (inset) exhibits the crystallinity of nanocrystals, and the lattice fringes match the (002) d spacing of QDs. For deposition of the multilayered QDs on the ITO/GO thin film, we employed a spin-assisted layer-by-layer assembled method by using the electrostatic interaction technique.[19] First, the as-synthesized QDs capped with oleic acid were surface-modified with cysteamine or mercaptopropinic acid to form NH_3^+-QDs and COO^--QDs dispersed in water which possess positive and negative charges on the surface of QDs, respectively. In addition, it was also found that the surface of GO thin film was usually negatively charged due to its containing oxygen functional groups.[20] The zeta potential measurements were thus performed to determine the surface charges of GO, NH_3^+-QD, and COO^--QD solutions at various pH values as shown in Figure 2c. The result showed that the surface of GO and COO^--QDs was negatively charged as the pH values change from 2 to 10 while the surface of NH_3^+-QDs was positively charged. As the pH value is increased from 2 to 10, the surface charges of GO were reduced, as a result of the ionization of the carboxylic acid and phenolic hydroxy groups attached in the GO.[21] In contrast, the surface of the NH_3^+-QDs becomes more positively charged as the solution is more acidic, which is mainly attributed to the amino group becoming ionic with the excess of hydrogen ion ($-H^+$) resulting in higher positive charges at lower pH value.[22] For the COO^--QDs, the zeta potentials were found to be more negatively charged with increasing pH values, where the proton of the carboxyl group was electrolytically dissociated to form a carboxylate anion ($-COO^-$).[23] Figure 2d shows the schematic illustration of the deposition of a QD multilayer structure using the electrostatic interactions among a GO thin film, NH_3^+-QDs and COO^--QDs. For the fabrication of ITO/GO thin film, the GO solution with a concentration of 8 mg/mL in DI water was prepared. By controlling the number of spin coating, we were able to obtain GO layers with different thicknesses. Then, the NH_3^+-QD solution with pH ~ 4 was utilized to be deposited on the GO thin film to form the first QD monolayer film (1 ML) by opposite electrostatic interaction.[19] After the deposition of each layer (GO and QD), the sample needed to be annealed at 150 °C under N_2 gas. Followed by two consecutive rinsing steps with deionized water (DI-water) to remove the free NH_3^+-QDs without electrostatic attraction on GO surface, the solution of COO^--QDs (pH ~ 10) with negative surface charges was spin-coated on top of the resulting ITO/GO/NH_3^+-QDs film and then rinsed by DI-water to form one bilayer film with two monolayers of QDs (2 MLs). Accordingly, the multilayered QD films (nMLs) can be prepared by following the spin-coating of NH_3^+-QDs and COO^--QDs alternately, where n represents the number of the deposited QD monolayer. Finally, the electron transporting layer of TPBi, LiF, and Al electrode was thus deposited on top of the QD active layer using a thermal evaporation method.

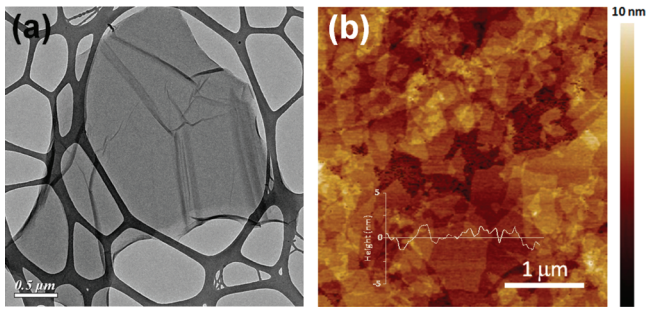

Figure 1. (a) TEM image of as-prepared GO sheet on a lacey carbon support. (b) AFM height images of GO thin film with thicknesses of approximately ~2 nm.

Next, we have employed Riken Keiki AC-2 photoelectron emission and Tauc plot[24] measurements to determine the

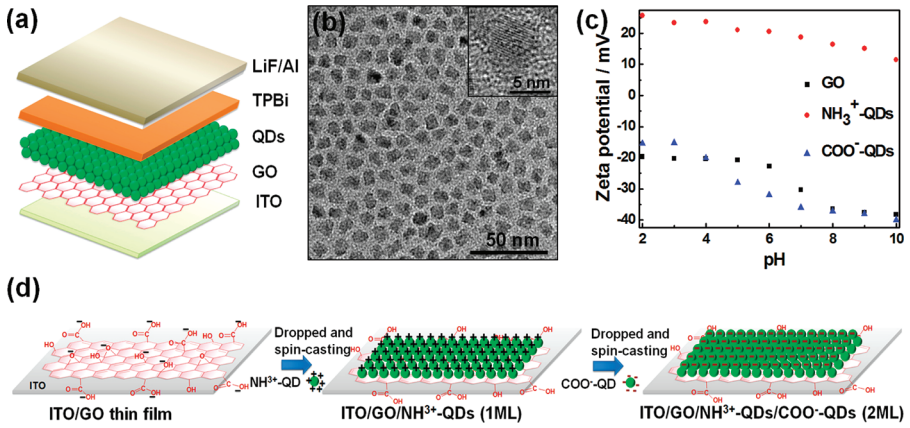

Figure 2. (a) QD-LEDs consisting of a device structure of ITO/GO/QDs/TPBi/LiF/Al. (b) TEM and high-resolution TEM (inset) images of CdSe/ZnS QDs. The average size of QDs is around ~7 nm ±1.5 nm. (c) Zeta potential of GO, NH_3^+-QD, and COO^--QD aqueous solution. (d) Schematic illustration of the layer-by-layer fabrication of QDs on the GO thin film.

highest occupied molecular orbital (HOMO) and the lowest unoccupied molecular orbital (LUMO) levels of GO thin films on ITO electrodes as shown in Figure 3a. The work function of the origin ITO electrode is around 4.7 eV. After depositing the GO films with different thickness of 2, 4, and 10 nm on ITO, the work functions of ITO/GO electrodes were increased to 5.17, 5.28, and 5.41 eV, respectively. The optical gap of GO can be obtained from the Tauc plot[24] using the relation $\alpha h\nu \propto (h\nu - E_g)^{1/2}$, where α is the absorption coefficient, $h\nu$ is the photon energy, and E_g is the optical gap. The Tauc plots for the 2, 4, and 10 nm thick GO films were shown in the inset of Figure 3b, indicating that the band gap of three GO thin films is around 3.6 eV. This value is comparable to the experimental band gap energy of the highly efficient NiO hole transport layer reported in ref 12. The relevant energetics of each component in the ITO/GO/QDs/TPBi/LiF/Al device are shown in Figure 3b.[4,17] The result indicated that GO thin films have a large band gap leading to hindering the possibility for electrons from the lowest unoccupied molecular orbital (LUMO) level of QDs to be collected at the ITO anode which reduces the electron–hole back recombination of the device. Figure 4a,b shows the current–voltage–luminescence (I–V–L) characteristics of the QD-LEDs with one monolayer QD (1 ML) with the deposition of GO hole transporting layers consisting of a thickness of 2, 4, and 10 nm, respectively. We found that the ITO-only device (no GO thin layer) exhibits a negligible luminescence efficiency of the QD-LED device with a large leakage current. No obvious diode behavior can be observed in this device (no shown), which is mainly originating from the possible direct contact between the TPBi layer and ITO substrate through vacancies in the QD thin film. The insertion of a 2 nm GO thin film between ITO and QDs results in a significant enhanced brightness and current density of 70 cd m^{-2} at 155 mA cm^{-2}. As the GO film thickness was further increased up to 10 nm, the device performances of the QD-LEDs show decreasing

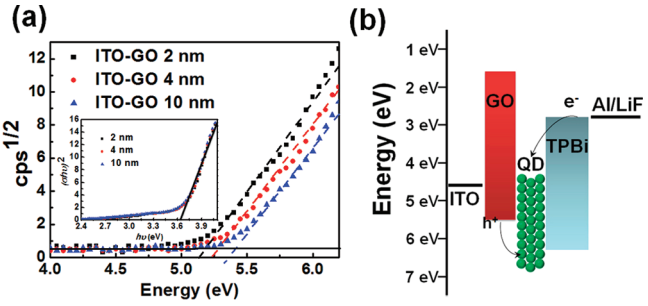

Figure 3. (a) Work function of ITO-GO films with different thickness films determined by Riken Keiki AC-2 photoelectron emission. The inset shows the Tauc plot measurement obtained from the absorption spectrum of GO. (b) Energy levels of the QD-LED device of this study. The average thickness of each GO thin film is 2 ± 0.3, 4 ± 0.4, and 10 ± 0.6 nm, respectively.

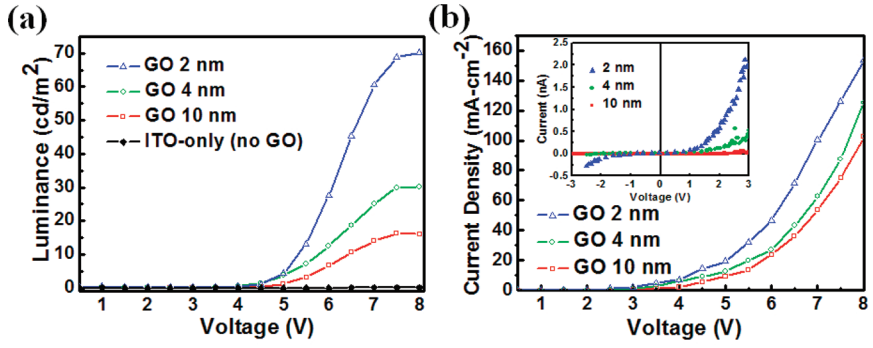

Figure 4. (a) Luminescence–voltage and (b) current–voltage characteristics of the QD-LEDs (1 ML) as a function of the thickness of GO thin films. The inset shows conductive-AFM current–voltage characteristics of the devices consisting of 2, 4, and 10 nm GO thin films on ITO substrates. The average luminance of devices are 70 ± 3, 30 ± 2, and 18 ± 2 cd/m^2 for 2, 4, and 10 nm GO thin film, respectively.

dx.doi.org/10.1021/jp210062x | J. Phys. Chem. C 2012, 116, 10181–10185

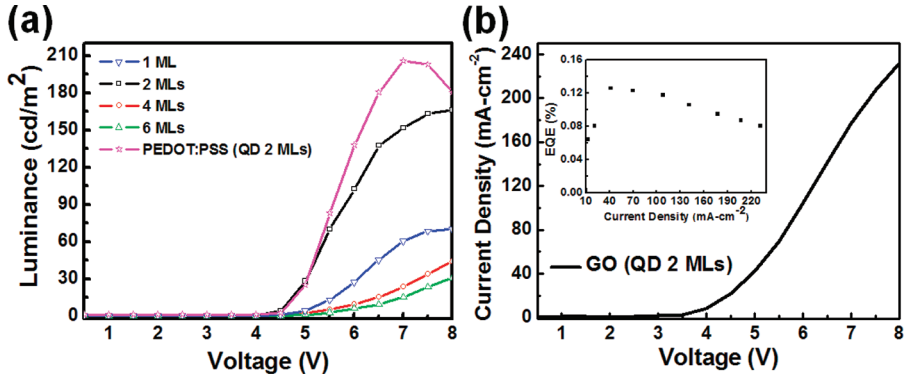

Figure 5. (a) Luminescence−voltage characteristics for the QD-LED devices with and different QD multilayers of n = 1, 2, 4, and 6 on top of the 2 nm GO thin film. The device with PEDOT:PSS was used as a referenced device. (b) Current−voltage characteristics for the QD-LED devices with the QD multilayer of n = 2. The inset shows the corresponding EQEs of the QD-LED device. The average luminance values of devices are 208 ± 5 cd/m^2, 165 ± 4 cd/m^2, 62 ± 3 cd/m^2, 45 ± 3 cd/m^2, and 30 ± 4 cd/m^2 for PEDOT, 2MLs, 1MLs, 4MLs, and 6MLs QDs, respectively.

luminescent efficiencies. Theoretically, the ITO-GO (10 nm) anode has a higher work function than the other two ITO-GO (4 and 2 nm) counterparts, which might be more probable to match the energy levels of QDs for enhancing the hole injection efficiently.[25] However, since GO is very insulating due to consisting of a high fraction of sp^3 carbon,[21] the increase in the thickness of GO thin films results in an increased serial resistance to slow down the carrier injection efficiency. The inset of Figure 4b shows the local current−voltage characteristics of the devices consisting of 2, 4, and 10 nm GO thin films onto the ITO electrodes, measured by the conductive atomic force microscope (AFM). It was found that the conductive current becomes largely suppressed from 2 to 0.06 nA at bias of 3 V as the thickness of the GO thin films increases from 2 to 10 nm. The above result shows that the thinnest insulating GO layer in the QD-LED thus acts as a most effective anode interfacial layer which favors holes to tunnel through and blocks electrons effectively.

To further optimize the brightness of devices, the QD-LEDs with different numbers of QD monolayers (nMLs) were thus deposited on top of the ITO/GO (2 nm) anode. Figure 5a shows the luminescence characteristics as a function of applied voltages for the QD-LED devices with different QD multilayers of n = 1, 2, 4, and 6. All the devices demonstrate a moderate turn-on voltage of ∼4.5 V. The device with 2 ML QD layer exhibits the maximum brightness of 165 cd m^{-2} at current density of 232 mA cm^{-2}. As the thickness of the QD layer was further increased, a drastic decrease in device performance in terms of brightness and current density can be observed, indicating that a thicker QD layer limits the EL efficiency with less efficient carrier transportation between different QDs.[26] Figure 5b exhibits the current density of the best performing device consisting of the 2 ML QD active layer deposited on top of the 2 nm GO thin film. The corresponding external quantum efficiencies of this QD-LED device as a function of injected current density were also shown in the inset. An external quantum efficiency of 0.08% was obtained for the maximum brightness (165 cd m^{-2} at 232 mA cm^{-2}, operated at an applied voltage of 8 V). We also used a PEDOT:PSS polymer to fabricate a referenced device which consists a device structure of ITO/PEDOT:PSS/QDs/TPBi/LiF/Al. The device using the PEDOT:PSS hole transporting layer and 2 ML QDs exhibits a higher brightness of 208 cd m^{-2} at a current density of 590 mA cm^{-2} but showed a lower external quantum efficiency due to its higher current density (see Supporting Information). Figure 6 shows the EL spectrum of this QD-LED device, showing an emission peak centered at 550 nm with a narrow full width at half-maximum (fwhm) of ∼35 nm. For comparison, the photoluminescence (PL) spectrum (red line) of the as-prepared QDs (excited by 325 nm UV light) was also shown. No obvious shift was observed in the spectral shape and peak position of the QD-LED device, indicating that the device emission is due entirely from QDs. The inset of Figure 6 shows the photographic image of the corresponding luminescent QD-LED device under operation.

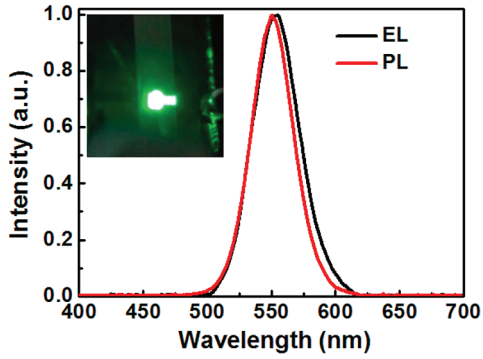

Figure 6. EL spectrum of the QD-LED device from Figure 4b. The PL spectrum of the QDs was also shown for comparison. The inset shows the photographic image of the luminescent QD-LED device.

4. CONCLUSION

In this work, we have demonstrated the incorporation of solution processable graphene oxide (GO) into QD-LEDs as the anode interfacial layer for hole transporting. We found that the QD-LED device consisting of the 2 ML QD active layer deposited on top of the 2 nm GO thin film showed the best luminescence performance (165 cd m^{-2} at 232 mA cm^{-2}, operated at an applied voltage of 8 V). The overall result showed that although the current device performance has not been fully optimized yet, the utilization of the solution processable GO thin film as the anode interfacial layer in the QD-LED device has offered the great potential of being compatible with the fabrication of solution processed printable optoelectronics. Further optimization in growing large area and uniform GO thin films should lead to additional improvements in the device performance as well as the stability.

■ ASSOCIATED CONTENT

Supporting Information

Additional figure. This material is available free of charge via the Internet at http://pubs.acs.org.

■ AUTHOR INFORMATION

Corresponding Author

*E-mail: chunwei@ntu.edu.tw (C.-W.C.); cjchen@ntnu.edu.tw (C.-C.C.).

Notes

The authors declare no competing financial interest.

■ ACKNOWLEDGMENTS

This work is supported by National Science Council, Taiwan (Project NSC 98-2119-M-002-020-, 99-2119-M-002-012-, and NSC 99-2120-M-003-001-).

■ REFERENCES

(1) Colvin, V. L.; Schlamp, M. C.; Alivisatos, A. P. *Nature* **1994**, *370*, 354−357.
(2) Coe, S.; Woo, W. K.; Bawendi, M.; Bulovic, V. *Nature* **2002**, *420*, 800−803.
(3) Steckel, J. S.; et al. *Angew. Chem., Int. Ed.* **2006**, *45*, 5796−5799.
(4) Zhao, J. L.; et al. *Nano Lett.* **2006**, *6*, 463−467.
(5) Cho, K. S.; et al. *Nat. Photonics* **2009**, *3*, 341−345.
(6) Bae, W. K.; Kwak, J.; Lim, J.; Lee, D.; Nam, M. K.; Char, K.; Lee, C.; Lee, S. *Nano Lett.* **2010**, *10*, 2368−2373.
(7) Anikeeva, P. O.; Halpert, J. E.; Bawendi, M. G.; Bulovic, V. *Nano Lett.* **2009**, *9*, 2532−2536.
(8) Tan, Z. N.; et al. *Nano Lett.* **2007**, *7*, 3803−3807.
(9) Lin, S. Y.; Tseng, C. C.; Lin, W. H.; Mai, S. C.; Wu, S. Y.; Chen, S. H.; Chyi, J. I. *Appl. Phys. Lett.* **2010**, *96*, 123503_1−123503_3.
(10) Ghosh, A. P.; Gerenser, L. J.; Jarman, C. M.; Fornalik, J. E. *Appl. Phys. Lett.* **2005**, *86*, 223503_1−223503_3.
(11) Caruge, J. M.; Halpert, J. E.; Bulovic, V.; Bawendi, M. G. *Nano Lett.* **2006**, *6*, 2991−2994.
(12) Caruge, J. M.; Halpert, J. E.; Wood, V.; Bulovic, V.; Bawendi, M. G. *Nat. Photonics* **2008**, *2*, 247−250.
(13) Schniepp, H. C.; et al. *J. Phys. Chem. B* **2006**, *110*, 8535−8539.
(14) Lerf, A.; He, H. Y.; Forster, M.; Klinowski, J. *J. Phys. Chem. B* **1998**, *102*, 4477−4482.
(15) He, H. Y.; Klinowski, J.; Forster, M.; Lerf, A. *Chem. Phys. Lett.* **1998**, *287*, 53−56.
(16) Eda, G.; Chhowalla, M. *Adv. Mater.* **2010**, *22*, 2392−2415.
(17) Li, S. S.; Tu, K. H.; Lin, C. C.; Chen, C. W.; Chhowalla, M. *ACS Nano* **2010**, *4*, 3169−3174.
(18) Lim, J.; Jun, S.; Jang, E.; Baik, H.; Kim, H.; Cho, J. *Adv. Mater.* **2007**, *19*, 1927−1932.
(19) Cho, J.; Char, K.; Hong, J.; Lee, K. *Adv. Mater.* **2001**, *13*, 1076−1078.
(20) Yang, F.; Liu, Y. Q.; Gao, L. A.; Sun, J. *J. Phys. Chem. C* **2010**, *114*, 22085−22091.
(21) Loh, K. P.; Bao, Q. L.; Eda, G.; Chhowalla, M. *Nat. Chem.* **2010**, *2*, 1015−1024.
(22) Hoshino, A.; Fujioka, K.; Oku, T.; Suga, M.; Sasaki, Y. F.; Ohta, T.; Yasuhara, M.; Suzuki, K.; Yamamoto, K. *Nano Lett.* **2004**, *4*, 2163−2169.
(23) Mori, K.; Kumami, A.; Yamashita, H. *Phys. Chem. Chem. Phys.* **2011**, *13*, 15821−15824.
(24) Tauc, J. *Mater. Res. Bull.* **1968**, *3*, 37−46.
(25) Armstrong, N. R.; Veneman, P. A.; Ratcliff, E.; Placencia, D.; Brumbach, M. *Acc. Chem. Res.* **2009**, *42*, 1748−1757.
(26) Sun, Q.; Wang, Y. A.; Li, L. S.; Wang, D. Y.; Zhu, T.; Xu, J.; Yang, C. H.; Li, Y. F. *Nat. Photonics* **2007**, *1*, 717−722.